Image Interpolation Algorithm for Edge Detection Using Directional Filters and Data Fusion

B.HIMABINDU
Asst.professor, Dept. of E.C.E, Chalapathi Institute of Technology, Guntur.

Abstract:
Preserving edge structures is a challenge to the image interpolation algorithms to reconstruct a high resolution image from a low resolution counterpart. We propose a new guide edge linear interpolation technique via address filter and data fusion. For a pixel to be interpolated, two sets of observation are defined in two orthogonal directions, and each set produces an estimated value of the pixel. These estimates of direction, following the model the different measures of the lack of noisy pixels are fused by linear least mean square estimation error (LMMSE) technique in a more robust estimate, and statistics two sets of observations. It also presents a simplified version of Based LMMSE interpolation algorithm to reduce computational cost without sacrificing much the interpolation performance. Experiments show that the new interpolation techniques can preserve sharp edges and reduce artifacts call.

Keywords: Bicubical convolution interpolation, Data Fusion, Edge preservation, Image interpolation, Laplacian, Linear Mean Square Estimation Error (LMMSE), optimal weight cubic interpolation.

1. Introduction

Many users of digital images desire to improve the native resolution offered by imaging hardware. Image Interpolation aims to reconstruct a higher resolution (HR) image of the associated low-resolution (LR) capture. You have medical imaging applications, remote sensing and digital Photos [3] - [4], etc. A number of image interpolation methods have been developed [1], [2], [4], [5], [7] - [15]. While commonly used linear methods such as duplication, pixel bilinear interpolation and bicubic interpolation convolution, have advantages in simplicity and fast implementation [7] who suffers from some inherent flaws, including the effects of block, blur the details and call artifacts around the edges. With the prevalence of low cost and relatively digital image LR devices and computing power increasingly interests and the demands of high quality, image interpolation algorithms have also increased. The human visual systems are sensitive to edge structures, to transmit a large part of the semantics of the picture, so that a re-key requirement for image interpolation algorithms to reconstruct faithfully the edges of the original scene. The traditional linear interpolation methods [1] - [3], [4] [5], does not work very well under the criterion of preserving the advantage. Some linear interpolation techniques [7] - [14] have been proposed in recent years to maintain Total sharpness. The interpolation scheme of Jensen and Anastassiou [7] detects the edges and adapts them for some templates to improve the visual perception of large images. Li and Orchard [8] uses the covariance of the estimate LR image covariance HR image, which represents the edge direction information to some extent, and proposed a Wiener filter-as the interpolation scheme. Since this method requires a relatively great window to calculate the covariance matrix for each offense sample, we can introduce some artifacts due to local structures statistics shows the change and, therefore, incorrect estimation of covariance. The interpolator of the image and Tenze Carrato [9] first replicates the pixels and then corrected by the use of some March 3 pre-edge patterns and optimizing the parameters of the operator. Muresan [14] detected no advantage in diagonal and diagonal addresses, and then recovered samples missing along direction detected by one-dimensional (1-D) polynomial interpolation.Some linear interpolation methods try to extend a image by predicting the fine structures of the image of human resources LR counterpart. For this, a multi-resolution representation image is needed. Takahashi and Taguchi [10] represents a Laplacian pyramid image, and with two empirically determine the parameters, it is estimated that the unknown high frequency components of the detail signal LR Laplacian. in the the last two decades, the wavelet transform (WT) theory [16] has been well developed and provides a good framework for multiresolution for the representation of the signal. WT decomposes signal different scales, along the sharp edges which have a signal correlation. Carey, et al. [11] exploits the Lipschitz property sharp edges of the scales of wavelets. Module is used Maximum thicker scales information to predict the unknown wavelet coefficients at the finer scale. Then the HR image is constructed by reverse WT. Muresan and Parks [13] extended this strategy through the influence of a full cone sharp edge in the wavelet scale space, rather than just the top module, for estimation of the best coefficients of scale through an optimal recovery theory. The wavelet interpolation method by Zhu et col. [12] uses a discrete time parametric model to characterize major edges. With this model in the wavelet domain lost information on the edge of the finest scale is recovered via minimum linear mean square estimation error (LMMSE). The previous schemes used, implicitly or explicitly, an isolated sharp edge model as an ideal step edge or softened,in the development of algorithms. For

real images, however, the wavelet coefficients of a sharp edge can be interfered with by the neighboring edges. In general, linear interpolation methods better advantage in preserving the linear methods. In [15], Guichard Malgouyres and analyzed some linear and nonlinear expanding imaging methods theoretically and experimentally. Compared with the discontinuities in the signals of 1-D, Ringer images of two dimensional (2-D) has an additional property: the direction. In the methods of linear interpolation, filtering is 1-D alternatively be made in horizontal and vertical directions without pay attention to the local edge structures. In the presence of a strong advantage if a sample is interpolated fault rather than artifacts from the direction of the edge, large and visually disturbing be introduced. A conservative strategy to avoid more serious devices is to use a 2-D isotropic filter. This, however, reduces the sharpness of the edges. A more "assertive" approach is to interpolate estimated edge in one direction. The problem with the latter is it worth the image quality is high if the estimated edge address is incorrect, which may occur due to difficulty in determining the direction of the edge of the paucity of data provided image by LR.In this paper we propose a new balanced approach to the problem. A sample is interpolated fault in not one but two orthogonal directions. The results are treated as two estimates of the sample and using the statistics fused adaptively a local window. Specifically, the partition of the neighborhood of each sample is missing in two orthogonal oriented subsets directions. The hope is that the observation of two sets exhibit different statistics, since the sample has missing higher correlation with its neighbors in the direction of the edge. Each oriented subset produces an estimate of the missing pixel. The finally pixel is interpolated by combining the two directional estimates on the principle of LMMSE. This process can discriminate the two subgroups according to their consistency absence of the sample, and make the subset perpendicular to the edge contribute less to address the LMMSE estimate of the missing shows. The new approach over a significant improvement the linear interpolation methods in preserving edge sharpness while the suppression of artifacts, by adapting the local interpolation gradient image. A drawback of the interpolation method proposed computational complexity is relatively high. Also interpolation algorithm to develop a simplified greatly reduced computing requirements, but without significant degradation in performance.

2. Edge-Guided Lmmse-Based Interpolation

We take a picture LR image F_t decreased from an image directly associated through human resources$F_h, F_l\ (n,m) = F_h\ (2n-1,2m-1), 1 \le n \le N, 1 \le m \le M$. Concerning the fig. 1, the black dots represent the samples available F_l and white dots represent samples missing from$F$.The problem of the interpolation is to estimate the missing samples F_h in HR image, whose size is 2N X 2M in the samples in LR F_l image whose size NXM.

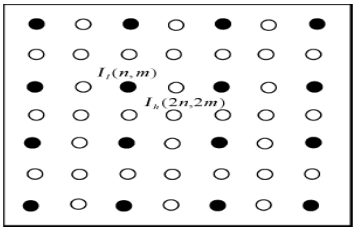

Fig. 1. Formation of an LR image from an HR image by directly down sampling.
The black dots represent the LR image pixels and the white dots represent the missing HR samples.

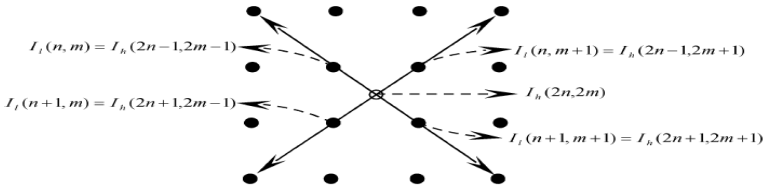

Fig. 2. Interpolation of the HR samples I_h *(2n, 2m)*.

Two estimates of I_h *(2n, 2m)* are made in the 45 and 135 directions as two noisy measurements of I_h *(2n, 2m)*.
The focus of the image interpolation is how to infer and use information about the shows that need to be hidden in neighboring pixels. If the sign of the sub-sampled LR image exceeds the Nyquist sampling, convolution-Methods based on interpolation will be affected by the alias problem in image reconstruction of human resources. This is the cause of artifacts such as ringing effects of image interpolation that are common to the linear interpolation methods. Given that the human visual system is very sensitive to the edges, especially in its spatial location is crucial to suppress interpolation artifacts, while retaining the sharpness

of the edges and geometry.The edge direction information is most important for the interpolation process. To extract and use this information, partitions of neighboring pixels of each sample of lack in two directional subsets are mutually orthogonal. In subset, a directional interpolation is done, and then the two interpolated values are merged to arrive at an estimate of LMMSE the sample is missing. We recover the HR image in two steps. First, the missing samples $F_h(2n, 2m)$ in the center locations surrounded by four samples are interpolated LR. Secondly, the other samples that is missing and is interpolated with the help of samples and recovered.

2.1. Interpolation of Samples $\mathbf{F_h\ (2n, 2m)}$

Referring to Fig. 2, we can interpolate the missing HR sample $F_h\ (2n, 2m)$ along two orthogonal directions: 45 diagonal and 135 diagonal. Denote by $\hat{F}_{45}\ (2n, 2m)$ and the $\hat{F}_{135}\ (2n, 2m)$ two results of interpolation direction from some of the linear methods, as bilinear interpolation, bicubic interpolation convolution [1] - [5]. Note the direction of interpolation results as noisy measurements of the sample failure HR

$$\hat{F}_{45}\ (2n, 2m) = F_h\ (2n, 2m) + u_{45}\ (2n, 2m)$$

$$\hat{F}_{135}(2n,2m) = F_h\ (2n, 2m) + u_{135}\ (2n, 2m) \quad (1)$$

where the random noise variables u_{45} and u_{135} represent the interpolation errors in the corresponding direction.
To fuse the two directional measurements $\hat{F}_{45}$ and $\hat{F}_{135}$ into a more robust estimate, we rewrite (1) into matrix form

$$Z = 1.F_h + U \quad (2)$$

Where

$$Z = \begin{bmatrix} \hat{F}_{45} \\ \hat{F}_{135} \end{bmatrix}, 1 = \begin{bmatrix} 1 \\ 1 \end{bmatrix} \text{ and } U = \begin{bmatrix} u_{45} \\ u_{135} \end{bmatrix}$$

Now, the interpolation problem is to estimate the unknown sample F_h from the noisy observation Z. This estimation can be optimized in minimum mean square-error sense. To obtain the minimum mean square-error estimation (MMSE) of F_h, i.e., $\hat{F}_h = E[F_h|Z] = \int F_h p(F_h|Z) dF_h$, we need to know the probability density function $p(F_h|Z)$. In practice, however, it is very hard to get this prior information or $p(F_h|Z)$ cannot be estimated at all. Thus, in real applications, LMMSE is often employed instead of MMSE. To implement LMMSE, only the first and second order statistics of F_h and Z are needed, which may be estimated adaptively.
From (2), the LMMSE of $F_h$can be calculated as [18]

$$\hat{F}_h = \mu_h + cov(F_h, Z)\big(Var(Z)\big)^{-1}(Z - E[Z]) \quad (3)$$

Where $\mu_h = E[F_h], Con(A, B) = E[(A - E[A])(B - E[B])^T]$ is the co-variance operator, and we abbreviate $Cov(A, A)$ as $Var(A)$, the variance operator. Through the LMMSE operation, $\hat{F}_h$ fuses the information provided by directional measurements $\hat{F}_{45}$ and $\hat{F}_{135}$.
Let $\mu_{45}^u = E[U_{45}], \mu_{135}^u = E[U_{135}]$. Through intensive experiments on 129 images, including outdoor and indoor images, portraits, MRI medical images, and SAR images, etc., we found that $\mu_{45}^u \approx 0$ and $\mu_{135}^u \approx 0$. Thus, noise vector U can be considered to be zero mean. Denote by n_1 and n_2 the normalized correlation coefficients of u_{45} and u_{135} with F_h.

$$n_1 = \frac{E[(u_{45} - \mu_{45}^u).(F_h - \mu_h)]}{\sqrt{E[(u_{45} - \mu_{45}^u)^2]E[(F_h - \mu_h)^2]}}$$

$$n_2 = \frac{E[(u_{135} - \mu_{135}^u).(F_h - \mu_h)]}{\sqrt{E[(u_{135} - \mu_{135}^u)^2]E[(F_h - \mu_h)^2]}}$$

Our experiments also show that the values of n_1 and n_2 are very small. Thus, we consider u_{45} and u_{135} and, consequently, U to be nearly uncorrelated with F_h. With the assumption that U is zero mean and uncorrelated with F_h, it can be derived from (3) that

$$\hat{F}_h = \mu_h + \sigma_h^2 1^T(1.\sigma_h^2.1^T + R_v)^{-1}(Z - \mu_h) \quad (4)$$

Where $\sigma_h^2 = var(F_h)$ and $R_V = Var(V)$.To implement the above LMMSE scheme for F_h, parametersμ_h, σ_h^2, and R_V need to be estimated for each sample $F_h(2n, 2m)$ in a local window.

First, let us consider the estimation of μ_h andσ_h^2. Again, referring to Fig. 2, the available LR samples around $F_h(2n, 2m)$ are used to estimate the mean and variance of $F_h(2n, 2m)$. Denote by W a window that centers at $F_h(2n, 2m)$ and contains the LR samples in the neighborhood of $F_h(2n, 2m)$. For estimation accuracy, we should use a sufficiently large window as long as the statistics is stationary in W. However, in a locality of edges, the image exhibits strong transient behavior. In this case, drawing samples from a large window will be counterproductive. To balance the conflicting requirements of sample size and sample consistency, we propose a Gaussian weighting in the sample window W to account for the fact that the correlation between $F_h(2n, 2m)$ and its neighbors decays rapidly in the distance between them. The further an LR sample is from$F_h(2n, 2m)$, the less it should contribute to the mean value of $F_h(2n, 2m)$. We compute μ_h as

$$\mu_h = \sum_l \sum_k W(l,k)\, G(l,k) \qquad (5)$$

Where $G(x,y) = (1/2\pi\zeta^2)\exp\left(-(x^2+y^2)/2\zeta^2\right)$ is a 2-D Gaussian filter with scale ζ. The variance of $I_h(2n, 2m)$ is computed as

$$\sigma_h^2 = \sum_l \sum_k (W(l,k) - \mu_h)^2\, G(l,k) \qquad (6)$$

Next, we discuss the estimation of R_V, the co-variance matrix of U. Using (1) and the assumption that u_{45} and u_{135} are zero mean and uncorrelated with F_h, it can be easily derived that

$$Var(u_{45}) = Var\left(\hat{F}_{45}\right) - \sigma_h^2$$
$$Var(u_{135}) = Var\left(\hat{F}_{135}\right) - \sigma_h^2 \qquad (7)$$

Since σ_h^2 has been estimated by (6), we need to estimate $var(\hat{F}_{45})$ and $var(\hat{F}_{135})$in a local window to arrive at $Var(u_{45})$ and $Var(u_{135})$ For this, we associate $\hat{F}_{45}$ with a set of its neighbors in the 45^0 diagonal direction. Denote by Y_{45} the vector that centers at $\hat{F}_{45}(2n, 2m)$

$$Y_{45} = \{\ldots, \hat{F}_{45}(2n+2, 2m-2), F_l(n+1, m), \hat{F}_{45}(2n, 2m)\, F_l(n, m+1), \hat{F}_{45}(2n-2, 2m+2), \ldots\} \qquad (8)$$

Set Y_{45} encompasses $\hat{F}_{45}$ and its neighbors, i.e., the original samples and the directional (45^0 diagonal) interpolated samples. Symmetrically, we define the sample set Y_{135} for $\hat{F}_{135}$ associated with interpolated results in the 135^0 diagonal

$$Y_{135} = \{\ldots, \hat{F}_{135}(2n-2, 2m-2), F_l(n, m), \hat{F}_{135}(2n, 2m) F_l(n+1, m+1), \hat{F}_{135}(2n+2, 2m+2), \ldots\} \qquad (9)$$

The estimates of $var(\hat{F}_{45})$ and $var(\hat{F}_{135})$ are computed as

$$var\left(\hat{F}_{45}\right) = \sum_k (Y_{45}(k) - \mu_h)^2 g(k)$$

and

$$var(\hat{F}_{45}) = \textstyle\sum_k (Y_{135}(k) - \mu_h)^2 g(k) \qquad (10)$$

Where $g(x) = (1/\sqrt{2\pi\xi})\exp\left(-x^2/2\xi^2\right)$ is a 1-D Gaussian filter with scaleξ.

Now, $Var(u_{45})$ and $Var(u_{135})$ can be computed by (8), and finally the co-variance matrix R_V can be estimated as

$$R_V = \begin{bmatrix} Var(u_{45}) & c_3 \cdot \sqrt{Var(u_{45}) Var(u_{135})} \\ c_3 \cdot \sqrt{Var(u_{45}) Var(u_{135})} & Var(u_{135}) \end{bmatrix} \qquad (11)$$

Where c_3 is the normalized correlation coefficient of u_{45} with u_{135}

$$c_1 = \frac{E[(u_{45} - \mu_{45}^u).(u_{135} - \mu_{135}^u)]}{\sqrt{E[(u_{45} - \mu_{45}^u)^2] E[(u_{135} - \mu_{135}^u)^2]}}$$

Although u_{45} and u_{135} are nearly uncorrelated with F_h, they are somewhat correlated to each other because $\hat{F}_{45}$ and $\hat{I}_{135}$ have some similarities due to the high local correlation. We found that the values of n_3 are between 0.4 and 0.6 for most of the test images. The correlation between u_{45} and u_{135} varies, from relatively strong in smooth areas to weak in active areas. In the

areas where sharp edges appear, which is the situation of our concern and interests, the values of n_3 are sufficiently low, and we can assume that u_{45} and u_{135} are uncorrelated with each other without materially affecting the performance of the proposed interpolation algorithm in practice. In practical implementationn_3, the correlation coefficient between u_{45} andu_{135}, can be set as 0.5 or even 0 for most natural images. Our experiments reveal that the interpolation results are insensitive ton_3. Varying n_3 from 0 to 0.6 hardly changes the PSNR value and visual quality of the interpolated image.If a sharp edge presents in F_h in or near one of the two directions (the 45^0 diagonal or the 135^0 diagonals), the corresponding noise variances $Var(u_{45})$ and $Var(u_{135})$ will differ significantly from each other. By the adjustment of R_V in (4), the interpolation value $\hat{F}_{45}$ or$\hat{F}_{135}$, whichever is in the direction perpendicular to the edge, will contribute far less to the final estimation result$\hat{F}_h$. The presented technique removes much of the ringing artifacts around the edges, which often appear in the interpolated images by cubic convolution and cubic spline interpolation methods.

2.2. Interpolation of samples $\mathbf{F_h(2n-1,2m)}$ and $\mathbf{F_h(2n,2m-1)}$

After the missing HR samples $\hat{F}_h(2n, 2m)$ are estimated, the other missing samples $F_h(2n-1,2m)$and $F_h(2n, 2m-1)$can be estimated similarly, but now with the aid of the just estimated HR samples. Referring to Fig. 3(a) and (b), the LR image pixels $F_t(n, m)$ are represented by black dots "●" while the estimated samples by symbols "⊗" The samples that are to be estimated are represented by white dots "○" As illustrated in Fig. 3, the missing sample $F_h(2n-1,2m)$or $F_h(2n, 2m-1)$ can be estimated in one direction by the original pixels of the LR image, and in the other direction by the already interpolated HR samples. Similar to (2), the two directional approximations of the missing sample are considered as the noisy measurements of $F_h(2n-1,2m)$and$F_h(2n, 2m-1)$, and then the LMMSE of the missing sample can be computed in a similar way as described in the previous section. Finally, the whole HR is reconstructed by the proposed edge-guided LMMSE interpolation technique.

3. Simplified Lmmse Interpolation Algorithm

In interpolating the HR samples, the LMMSE technique of (4) needs to estimateμ_h, σ_h^2, R_V, and compute the inverse of a 2X2 matrix. This may amount to too heavy a computation burden for some applications that need high throughput. Specifically, if we set μ_h be the average of the four nearest LR neighbors of F_h to reduce computation, then computing μ_h needs three additions and one division and computing σ_h^2 needs seven additions, four multiplications, and one division. By setting the size of vector Y_{45} and Y_{135} as 5 and setting $R_V = diag\{Var(u_{45})$ and $Var(u_{135})\}$, i.e., $n_3 = 0$, in (10) to reduce the computational cost, we still need 20 additions and 20 multiplications to compute R_V. The remaining operations in (4) include nine additions, eight multiplications, and one division. In total, the algorithm needs 39 additions, 32 multiplications, and three divisions to compute a $\hat{F}_h$ with (4).One way to reduce the computational complexity of the algorithm is invoked judiciously LMMSE only for pixels where high local activities are detected, and use a simple linear interpolation method in smooth regions. Since edge pixels represent the minority of the total population of the sample, this will result in significant savings in the calculations. Furthermore, a simplified version of the algorithm based on LMMSE interpolation while only slightly decreasing the performance.We can see that the LMMSE estimate of HR sample I_h is actually a linear combination of $\hat{F}_{45}$, $\hat{F}_{135}$ and μ_h. Referring to (4) and let $\Gamma = \sigma_h^2 1^T(1.\sigma_h^2.1^T + R_V)^{-1}$, then Γ is a 2-D vector and we rewrite (4) as

$$\hat{F}_h = \Gamma_1.\hat{F}_{45} + \Gamma_2.\hat{F}_{135} + (1 - \Gamma.1)\mu_h \quad (12)$$

Where Γ_1 and Γ_2 are the first and second elements of Γ. We empirically observed that $(1 - \Gamma.1)$ is close to zero, and, hence, μ_h has a light effect on $\hat{F}_h$. In this view, $\hat{F}_h$ can be simplified to a weighted average of $\hat{F}_{45}$ and $\hat{F}_{135}$, while the weights depend largely on the noise covariance matrix R_V.

Instead of computing the LMMSE estimate of F_h, we determine an optimal pair of weights to make $\hat{F}_h$ a good estimate of F_h. The strategy of weighted average leads to significant reduction in complexity over the exact LMMSE method. Let

$$\hat{F}_h = w_{45}.\hat{F}_{45} + w_{135}.\hat{F}_{135} \quad (13)$$

Where $w_{45} + w_{135} = 1$. The weights w_{45} and w_{135} are determined to minimize the mean square-error (MSE) of $\hat{F}_h$:

$\{w_{45}, w_{135}\} = arg\ \min_{w_{45}+w_{135}=1} E[(\hat{F}_h - F_h)^2]$.

Although the measurement noises of $\hat{F}_{45} and\ \hat{F}_{135}$, i.e., u_{45} and u_{135} , are Correlated to some Extent, Their correlation is Sufficiently low to Consider u_{45} and u_{135} as being approximately uncorrelated. This assumption holds better in the areas of Edges That Are Critical to the human visual system and of interests to us. In fact, if u_{45} and $u_{135}$are highly Correlated, That is to say, the two estimates $\hat{F}_{45} and\ \hat{F}_{135}$ are close to each other, then F_h varies little in w_{45} and w_{135}anyway. With the assumption That u_{45} and $u_{135}$are approximately uncorrelated, we can show the optimal weights are That

$$w_{45} = \frac{var(u_{135})}{var(u_{45})+var(u_{135})},\ w_{135} = 1 - w_{45} \quad (14)$$

It is quite intuitive why weighting system works. For example, for an edge in or near the 135 ° diagonal direction, the variance Var (u_{45}) is greater than var (u_{135}). Of (14), which is smaller than $w_{45}$and w_{135}will therefore have less influence F_{45} in F. $\hat{F}_{135}$, and vice versa. To calculate var (u_{45}) and var (u_{135}) as described in Section II, however, we still have 30 additions, 24 multiplications and divisions, two. In order to simplify and speed up the calculation of $w_{45}$and w_{135}, we use the following approximations: $var(u_{45}) \cong (\sum_{k=1}^{5}|Y_{45}(k) - \mu_h|)^2$

$$var(u_{135}) \cong \left(\sum_{k=1}^{5}|Y_{135}(k) - \mu_h|\right)^2 \quad (15)$$

where "≅" is almost equivalent. With the above simplification, we only need 23 additions, multiplications and divisions to two, two to get w_{45} and w_{135}. Finally, with (13), only need 24 additions, multiplications and divisions of four, two to get $\hat{F}$. This results in significant savings compared with computational (4), which requires 39 additions, 32 multiplications and divisions, three. Table I shows the counts of the algorithm and the algorithm simplified LMMSE.

TABLE I
Operations needed for the LMMSE algorithm
And the simplified algorithm

Operation	Addition	Multiplication	Division
LMMSE algorithm	39	32	3
Simplified algorithm	24	4	2

4. Experimental Results

The proposed interpolation algorithms were implemented and tested, and their performance was compared to some existing methods. We welcome some images of human resources for the corresponding LR images, of which the original images were reconstructed human resources by the proposed methods and competitive. Since the original images of HR are known in the simulation, we compare the results with real images interpolated, and measure the PSNR of the interpolated images. The interpolator based LMMSE introduced was compared with bicubic convolution interpolation, bicubic spline interpolator, the subpixel edge detection based Anastassiou interpolator and Jensen [7], and the Wiener-like filter interpolator Orchard Li and [8]. To assess the sensitivity of the proposed interpolation algorithms for different initial estimates of management before the merger, which were tested when combined with interpolators bicubic and bilinear convolution, respectively. In the figure legends, the LMMSE method developed in Section II is labeled LMMSE_INTR_linear LMMSE_INTR_cubic or, depending on whether or bilinear bicubic convolution interpolation is used to obtain an initial estimate of direction. Similarly, the simplified method of Section III is labeled OW_INTR_cubic (OW represents the optimal weight) or OW_INTR_linear. In the experiments, sets the scale of 2-DG ζ Gaussian filter [referring to (5)] around 1 and ξ scale of1-D Gaussian filter g [referring to (9)] in about 1.5. Our experimental results also draw attention to a fact that the proposed methods are insensitive to the choice of initial directional interpolators. Even with bilinear interpolation, which normally get significantly worse results than bicubic interpolation, the end result is merged very close to that of bicubic interpolation, especially in terms of visual quality. Figs. 3 and 4 show the interpolated images butterfly Lena and LMMSE_INTR_cubic and LMMSE_INTR_linear methods. In visual effects, the two methods are almost indistinguishable. This shows the power of LMMSE strategy based on data fusion in correcting much of interpolation errors of traditional linear methods.

(a)

(b)

Fig.3. Interpolated image Lena by (a) LMMSE_INTR_cubic and (b) LMMSE_INTR_linear.


(a)


(b)

Fig.4. Interpolated image *Butterfly* by
(a) LMMSE_INTR_cubic and (b) LMMSE_INTR_linear.


(a)


(b)


(c)


(d)


(e)


(f)

Fig.5. Interpolation results of the image *Lena*. (a)Original image, interpolated image by (b) the cubic convolution, (c)the method in [8], (d) the method in [9],(e)the proposed LMMSE_INTR_cubic, and (f) the proposed OW_INTR_cubic.

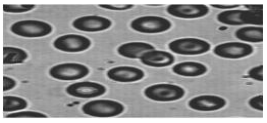
(a)

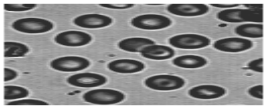
(b)

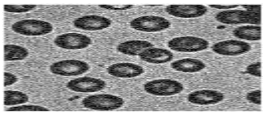
(c)

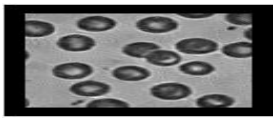
(d)

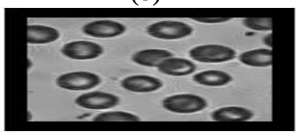
(e)

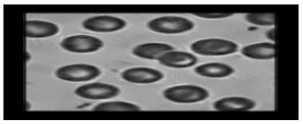
(f)

Fig.6. Interpolation results of the image blood. (a) Original image, interpolated image by (b) the cubic convolution, (c) the method in [8], (d) the method in [9],(e) the proposed LMMSE_INTR_cubic, and (f) the proposed OW_INTR_cubic.


(a)


(b)

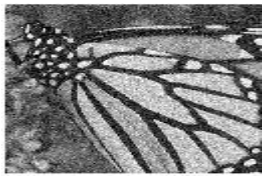
(c)


(d)

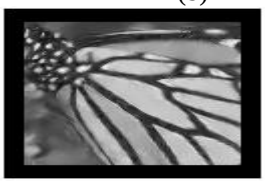
(e)

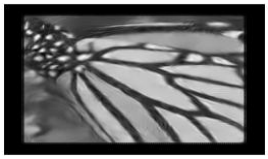
(f)

Fig.7. Interpolation results of the image butterfly. (a) Original image, interpolated image by (b) the cubic convolution, (c) the method in [8], (d) the method in [9],(e) the proposed LMMSE_INTR_cubic, and (f) the proposed OW_INTR_cubic.

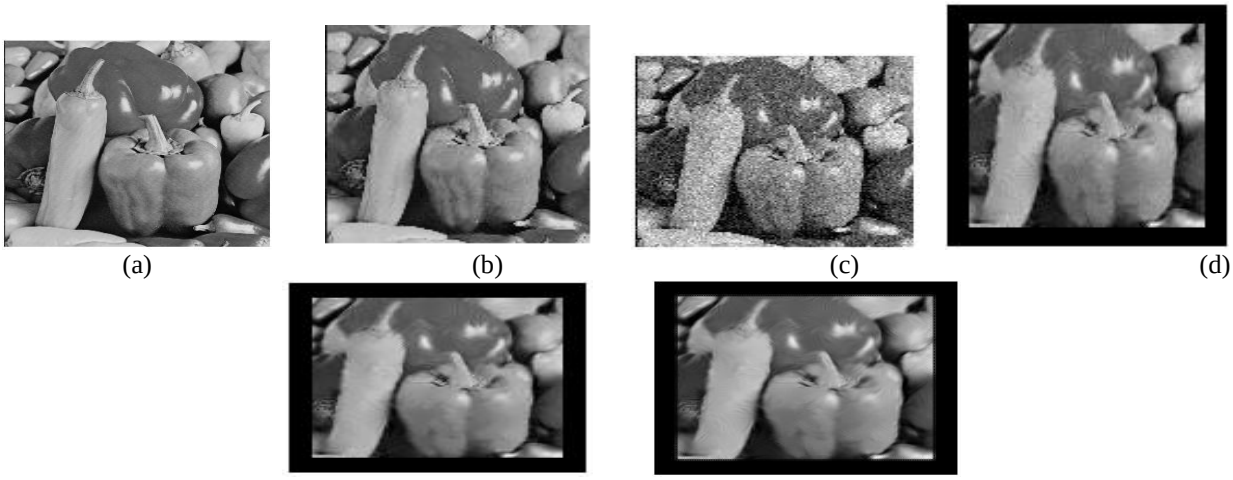

(a) (b) (c) (d)

(e) (f)

Fig.8. Interpolation results of the image peppers. (a) Original image, interpolated image by (b) the cubic convolution, (c) the method in [8], (d) the method in [9],(e) the proposed LMMSE_INTR_cubic, and (f) the proposed OW_INTR_cubic.

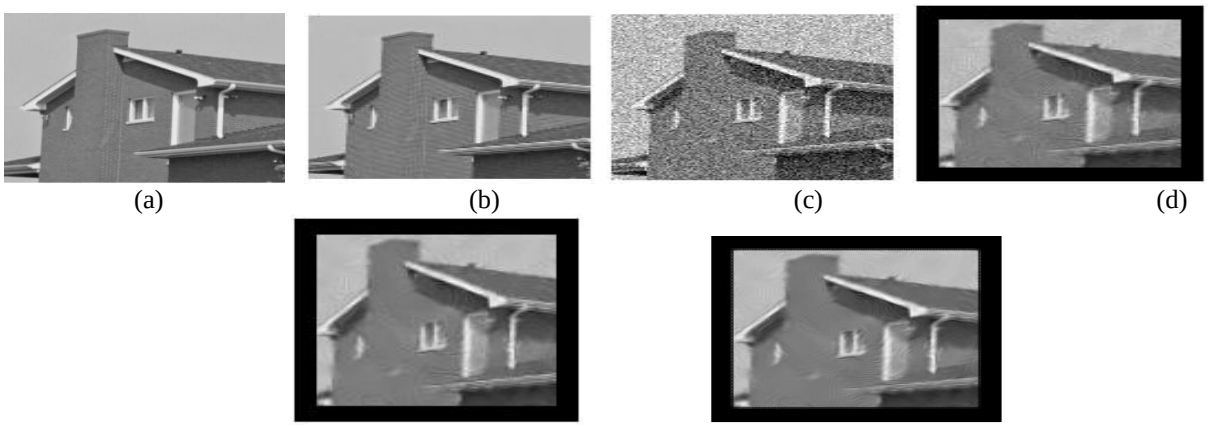

(a) (b) (c) (d)

(e) (f)

Fig.9. Interpolation results of the image house. (a) Original image, interpolated image by (b) the cubic convolution, (c) the method in [8], (d) the method in [9],(e) the proposed LMMSE_INTR_cubic, and (f) the proposed OW_INTR_cubic.

In Figs. 5-9, we compare the visual quality of the test interpolation methods for natural images: Lena, blood samples, butterfly, Peppers, and house. The proposed methods remove many of the ringing and other visual artifacts of the other methods. The OW_INTR_cubic method is slightly inferior to the LMMSE_INTR_cubic method in reducing the ringing effects, but this is a small price to pay for the computational savings of the former. The interpolator of Jensen and Anastassiou [7] can reproduce very thin edges in the object contour because it contains a subpixel edge detection process, but it causes visible artifacts when the edge detector commits errors.This method leaves a considerable amount of ringing effects in the hat of Lena and the wing of the Butterfly. The interpolator of Li and Orchard [8] can preserve large edge structures well, such as those in Lena; however, it introduces artifacts in the finer edge structures, such as the drops of Splash and the head part of Butterfly. Another disadvantage of Li and Orchard's method is its high computational complexity. If an 8x8 window is used to compute the covariance matrix, this algorithm requires about 1300 multiplications and thousands of additions. In comparison, the proposed LMMSE_INTR_cubic algorithm requires only tens of multiplications and divisions. The down-sampling process considered in this paper, through which an LR image is generated from the corresponding HR image, is ideal Dirac sampling. An alternative model of LR images is that of low-pass filtering followed by down-sampling.

5. Conclusion

We have developed an edge type guided LMMSE image interpolation technique. For each pixel to be interpolated, the partition of their neighborhood into two subsets of observation in two orthogonal directions. Each subset observation was used to generate an estimate of the missing sample. These two directional estimates were processed as two sample noisy measurements missing. Using statistics and combination of the two subsets of observation merged the two measurements of noise in a more robust estimation through linear minimum mean square estimation error. To reduce the computational complexity of the proposed method was simplified to an optimal weighting problem and determines the optimum weights. The simplified method had a competitive performance with significant computational savings. The experimental results showed that the methods presented avoided interpolation against edge directions and, therefore, achieve remarkable reduction in timbre and other visual artifacts.

Referance

[1] H. S. Hou, "Cubic splines for image interpolation and digital filtering,"*IEEE Trans. Acoustic, Speech, Signal Process.*, vol. ASSP-26, no. 6,pp. 508–517, Dec. 1978.

[2] R. G. Keys, "Cubic convolution interpolation for digital image processing," *IEEE Trans. Acoustic, Speech, Signal Process.*, vol.ASSP-29, no. 6, pp. 1153–1160, Dec. 1981.

[3] T. M. Lehmann, C. Gönner, and K. Spitzer, "Survey: Interpolation methods in medical image processing," *IEEE Trans. Med. Imag.*, vol.18, no. 11, pp. 1049–1075, Nov. 1999.

[4] M. Unser, "Splines: A perfect fit for signal and image processing,"*IEEE Signal Process. Mag.*, no. 11, pp. 22–38, Nov. 1999.

[5] M. Unser, A. Aldroubi, and M. Eden, "Enlargement or reduction of digital images with minimum loss of information," *IEEE Trans. Image Process.*, vol. 4, no. 3, pp. 247–258, Mar. 1995.

[6] B. Vrcelj and P. P. Vaidyanathan, "Efficient implementation of all-digital interpolation," *IEEE Trans. Image Process.*, vol. 10, no. 11, pp.1639–1646, Nov. 2001.

[7] K. Jensen and D. Anastassiou, "Subpixel edge localization and the interpolation of still images," *IEEE Trans. Image Process.*, vol. 4, no. 3,pp. 285–295, Mar. 1995.

[8] X. Li and M. T. Orchard, "New edge-directed interpolation," *IEEE Trans. Image Process.*, vol. 10, no. 10, pp. 1521–1527, Oct. 2001.

[9] S. Carrato and L. Tenze, "A high quality 2_image interpolator," *IEEE Signal Process. Lett.*, vol. 7, no. 6, pp. 132–135, Jun. 2000.

[10] Y. Takahashi and A. Taguchi, "An enlargement method of digital images with the predition of high-frequency components," in *Proc.Int. Conf. Acoustics, Speech, Signal Processing*, 2002, vol. 4, pp.3700–3703.

[11] W. K. Carey, D. B. Chuang, and S. S. Hemami, "Regularity –Preserving image interpolation," *IEEE Trans. Image Process.*, vol. 8, no. 9, pp.1293–1297, Sep. 1999.

[12] Y. Zhu, S. C. Schwartz, and M. T. Orchard, "Wavelet domain image interpolation via statistical estimation," in *Proc. Int. Conf. Image Processing*,2001, vol. 3, pp. 840–843.

[13] D. D. Muresan and T. W. Parks, "Prediction of image detail," in *Proc.Int. Conf. Image Processing*, 2000, vol. 2, pp. 323–326.

[14] D. D. Muresan, "Fast edge directed polynomial interpolation," in *Proc.Int. Conf. Image Processing*, 2005, vol. 2, pp. 990–993.

[15] F. Malgouyres and F. Guichard, "Edge direction preserving image zooming: A mathematical and numerical analysis," *SIAM J. Numer.Anal.*, vol. 39, pp. 1–37, 2001.

[16] S. Mallat, *A Wavelet Tour of Signal Processing*. New York: Academic,1999.